PHYSICAL REVIEW A VOLUME 28, NUMBER 4 OCTOBER 1983

# Resonance and intermediate-coupling effects in electron scattering with highly charged ions. I. Collision strengths for $Fe^{24+}$, $Se^{32+}$, and $Mo^{40+}$

A. K. Pradhan*
*Department of Physics, University of Windsor, Windsor, Ontario N9B 3P4, Canada*
(Received 15 April 1983)

A study of electron-impact excitation of highly charged ions in the helium isoelectronic sequence is reported. Nonresonant, intermediate-coupling collision strengths are computed for transitions up to and including the $n=3$ states. With the 13 fine-structure levels, i.e., $1s^2(^1S_0)$, $1s\,2s(^3S_1;^1S_0)$, $1s\,2p(^3P_{0,1,2};^1P_1)$, $1s\,3s(^3S_1;^1S_0)$, and $1s\,3p(^3P_{0,1,2};^1P_1)$, there are 78 different inelastic transitions. Main calculations are carried out in the nine-state distorted-wave approximation including partial waves $l \leq 15$. Relativistic effects are taken into account in the Breit-Pauli approximation. Nine-state close-coupling calculations are also carried out for $Fe^{24+}$ with $l \leq 4$ at a few energies for comparison (and for later work in paper II). Higher partial waves ($l > 15$) are treated by the Coulomb-Bethe method using accurate relativistic eigenenergies and oscillator strengths for the target ions. The $Z$ dependence of the departure from $LS$ coupling is investigated. Present results are in good general agreement with previous calculations where available, but some discrepancies are noted or clarified. Collision strengths are tabulated at energies from near the excitation energy of the $n=3$ complex to sufficiently high energies to enable rate coefficients to be computed. For transitions to the $n=3$ levels and for transitions where resonances are not important, the present values should yield reasonably accurate excitation rates (resonances are considered in paper II). The present data are required particularly for the analysis of observed spectra from high-temperature, high-density plasmas where the line intensities may depend on collisional redistribution among a number of excited $n=2$ and $n=3$ states.

## I. INTRODUCTION

Even as the need for large scale computation of atomic data remains substantially unfulfilled, the requirement for a high degree of accuracy in such calculations has become imperative in order to analyze the very high-resolution observations of laboratory and astrophysical plasmas that are now possible and are being made. In particular, one may cite the recent work in the x-ray spectroscopy of the solar corona[1] and tokamak plasmas[2,3] where the high temperature leads to nearly complete ionization of certain medium heavy elements ($Z > 15$). Line spectra of these trace ions provide a valuable tool for the diagnostics of plasma parameters; however, accurate rates are required for a number of atomic processes, such as electron-impact excitation, radiative and dielectronic, recombination, cascades, etc. Calculations for the excitation and recombination rates are particularly difficult since the most advanced methods depend on rather huge investment of computing time and manpower. For highly charged ions the problem at first appears to be simpler but it has now become clear that certain important atomic effects manifest themselves as one approaches $Z > 20$. In our earlier work on electron excitation of heliumlike ions[4] it was shown that resonances play an important role in the scattering process enhancing the cross sections by several factors for some important transitions. The ions considered ranged from $Be^{2+}$ to $Fe^{24+}$. These calculations (to be referred to as PNH) were carried out in $LS$ coupling although it was realized that for Fe (and, to a small extent, Ca), some cross sections would exhibit fine-structure effects. Subsequent work[5] also revealed that the large resonance structures present in the cross sections would also be susceptible to radiative decay which would compete with autoionization and lead to dielectronic recombination (DER). It was shown that in some energy ranges, particularly in the region just below the threshold where the resonances converge, the effect of DER could be considerable. As the radiative transition probabilities increase as $Z^4$ (for allowed transitions), one must take DER into account for heavy elements such as iron. Thus, while the other criteria for accurate scattering calculations (e.g., an optimum eigenfunction expansion) still apply, the task for highly charged, heavy ions also involves the full consideration of (i) departure from $LS$ coupling, (ii) autoionization enhancement, and (iii) reduction in autoionization due to DER.

The present work is divided into two parts: papers I and II. The first part is concerned with the calculation of intermediate-coupling (IC) collision strengths for all transitions, including the fine structure, that result from a nine-state target expansion in $LS$ coupling. The 13 fine-structure states are $1s^2(^1S_0)$, $1s2s(^3S_1;^1S_0)$, $1s\,2p(^3P_{0,1,2};^1P_1)$, $1s\,3s(^3S_1;^1S_0)$, and $1s3p(^3P_{0,1,2};^1P_1)$. IC collision strengths are computed for all transitions in the energy region above $E(n=3)$, where no resonances are taken into account. The second part deals with autoionization and DER effects that are described in detail in the energy range between the $n=2$ and the $n=3$ states. For transitions involving the $n=2$ levels, the final collision

 

strengths are as computed in papers I and II, whereas collision strengths for transitions to the $n=3$ states are given in paper I. Three different ions in the helium sequence are considered: $Fe^{24+}$, $Se^{32+}$, and $Mo^{40+}$, in order to study the $Z$ dependence of the collision strengths. Also, since it is not possible to carry out such extensive calculations for many ions, it is hoped that $Z$ interpolation and extrapolation would provide fairly accurate estimates for ions not included in this study. Nine-state distorted-wave (9DW) and nine-state close-coupling (9CC) approximations are employed in the calculations, the former with partial waves $l,l' \leq 15$ and the latter with $l,l' \leq 4$. This was done mainly as a check for any detailed difference between the two that may be evident for low partial waves and if so, to use the more accurate 9CC reactance matrices for resonance analysis, particularly for extrapolation with the multichannel quantum-defect theory (MCQDT). Higher partial waves $l,l' > 15$ were summed over in the Coulomb-Bethe (CB) approximation. In this work we describe some general theoretical and computational techniques to compute cross sections for very highly charged ions. In addition, we aim to "complete" the calculations for the high-$Z$ He-like ions, with the atomic effects mentioned above, that were not included by PNH. In Sec. IV of this paper, the nonresonant IC collision strengths are compared with earlier available results and reasonably good agreement is found. In paper II we find that for a few transitions both the IC and the resonance effects are very important and for many others the resonances make a large contribution to the cross sections. No previous calculations have dealt with all the three effects (IC, autoionization, and DER).

## II. THEORY AND METHOD

The theory for scattering calculations in the CC and the DW methods is described elsewhere.[6-8] Here we sketch, very briefly, the outline of the basics together with the computational techniques developed by Eissner, Jones, and Nussbaumer[9] and Saraph[10] in order to take account of relativistic effects and for transformation from the $LS$ to an IC scheme. The treatment of resonances forms an extension of these methods and is described in paper II.

In both the CC and the DW approximations the total ($e$ plus ion) wave function is expanded into target eigenstates plus a set of bound-state wave functions:

$$\Psi^{SL\pi} = \sum_{i=1}^{NF} \theta_i + \sum_{j=1}^{NB} c_j \Phi_j \ , \tag{1a}$$

$$\theta_i = A[\phi(S_i L_i) F_i(r,k_i^2)] \ . \tag{1b}$$

where the $\theta_i$ is an antisymmetrized product of the wave function for an ionic state $S_iL_i$ with the orbital function of the scattering electron, and $\Phi_j$ is an $(N+1)$ electron bound-state wave function introduced primarily due to orthogonalization of the one-electron target wave functions and the scattering electron wave function. However, the set $\{\Phi_j\}$ may also include bound-state functions to provide additional short-range correlation for the functions in the first sum in Eq. (1a). The channel terms in Eq. (1b) may be "open" or "closed" according to whether the kinetic energy of the colliding electron is higher or lower than the target state to which it is coupled: i.e., if the target term is labeled $S_iL_i$ then the channel is open or closed according to whether $[k(S_iL_i)]^2$ is less than or greater than $E(S_iL_i)$. The radial functions $F_i(r)$ and the coefficients $c_j$ may be varied to satisfy the Kohn variational principle, leading to a set of coupled integro-differential (ID) equations for the CC approximation and to a "corrected" reactance matrix $\underline{R}^{\rm DW}$ in the DW approximation. As pointed out, first by Hayes and Seaton,[11] and by PNH, the functions $\Phi_j$ automatically result in resonances in the $\underline{R}$ matrix. For the DW approximation we may express the $\underline{R}$ matrix elements as

$$R_{ii'}^{\rm DW} = -\{F_i \mid (h_i - k_i^2)\delta_{ii'} + [\underline{W} - \underline{U}^{\dagger}(\mathscr{H}-E)^{-1}\underline{U}]_{ii'} \mid F_{i'}\} \ , \tag{2}$$

where $h_i$ is the one-electron Hamiltonian operator and $\underline{W}$ and $\underline{U}$ are potential operators. The radial distorted wave functions are computed in a statistical model potential of the Thomas-Fermi-Dirac type. The pole positions in the DW calculations then lie precisely at the eigenvalues of the functions $\Phi_j$,

$$\mathscr{H}_{jj'} = \langle \Phi_j \mid H \mid \Phi_{j'} \rangle \delta_{jj'} \ . \tag{3}$$

In the CC calculations the pole positions are somewhat different from (3) due to additional correlation between the closed and bound channels. The coupled ID equations are solved at the incident energies of the scattering electron to yield $\underline{R}^{\rm CC}$. The point to note is that, in the work of PNH, resonances may thus be accounted for in the DW approximation which does not allow for coupling between channels, unlike the CC approximation where the coupling between open and closed channels leads to resonances.

The first problem in scattering calculations is the accurate determination of the target eigenfunctions $\phi(S_iL_i)$. In order that the computations may remain tractable, only a few such states can practically be considered. However, configuration interaction requires at least some other higher states to be included. The general purpose techniques for the calculation of atomic parameters developed by Eissner *et al.*[9] are used to obtain the necessary target representation and radiative data. The central-field potential employed by Eissner *et al.* is of Thomas-Fermi-Dirac—type with adjustable parameters usually varied to optimize target energies and radiative quantities. Collision strengths are then obtained by the DW or the CC methods. However, these are in the $LS$ coupling scheme which for highly ionized atoms, where relativistic effects become prominent, is no longer valid. Eissner *et al.* treat the relativistic problem in the Breit-Pauli approximation and thereby compute the atomic data with the fine structure. The relativistic correction operators in the Breit-Pauli Hamiltonian include the following: (i) one-body terms for mass variation, Darwin correction, and the spin-orbit interaction, (ii) two-body fine-structure terms for spin-other orbit and spin-spin interactions, and (iii) two-body nonfine-structure terms for spin-spin contact, the two-body Darwin term, and the orbit-orbit interaction. Eissner *et al.* exclude the two-body nonfine-structure

terms (iii) from consideration; this has little effect on the collision problem (see Jones[12]), although the eigenenergies for some fine-structure states in highly ionized ions exhibit slight but significant variations.

The fine-structure collision strengths are obtained from the *LS* coupled ones, through transformation of the $\underline{R}$ matrices from *LS* to IC, using term-coupling coefficients derived by the method of Eissner *et al.* discussed above. The transformation is accomplished by an approach used by Saraph[10] and is sketched below. First, a purely algebraic transformation is carried out to a pair-coupling scheme,

$$S_i + L_i = J_i, \quad J_i + l = K$$

and (4)

$$K + s = J ,$$

where $l$ and $s$ are the orbital and spin momenta of the colliding electron, $J_1$ is the target fine-structure state, and $J$ is the total ($e$ plus ion) angular momentum. The reactance matrices in the two representations are related as

$$\underline{R}^{J\pi}(S_i L_i J_i K; S_i' L_i' J_i' l' K') = \sum_{S,L} X(SLJ, S_i L_i J_i, lk) R^{SL\pi}(S_i L_i l s; S_i' L_i' l' s') \times X(SLJ, S_i' L_i' J_i'; l' K') , \quad (5)$$

where the $X$ are products of Racah recoupling coefficients. The second step is to transform the $\underline{R}^{J\pi}$ to allow for intermediate term coupling in the target, i.e.,

$$R^{J\pi}(\Delta_i J_i l K, \Delta_i' J_i' l' K') = \sum_{\substack{S_i, L_i \\ S_i', L_i'}} t_{J_i}(\Delta_i, S_i L_i) R^{J\pi}(S_i L_i J_i l K; S_i' L_i' l' K') \times t_{J_{i'}}(\Delta_i, S_i' L_i') , \quad (6)$$

where the $t_{J_i}$ are term-coupling coefficients defined in terms of the configuration mixing coefficients for *LS* coupling, $a_{S_i L_i}$ (which diagonalize the nonrelativistic Hamiltonian), and the mixing coefficients $b_{J_i}$ for diagonalizing the Breit-Pauli Hamiltonian ; i.e.,

$$t_{J_i}(\Delta_i, \Gamma_i S_i L_i) = \sum_{C_i \beta_i} a^{S_i L_i}(\Gamma_i, C_i \beta_i) b^{J_i}(\Delta_i, C_i \beta_i S_i L_i) , \quad (7)$$

where the $\Gamma_i$ labels a term composed of several configurations $C_i$, and $\beta_i$ is a degeneracy parameter for more than one *LS* term due to $C_i$. The accuracy of the coefficients $t_{J_i}$ is dependent on the target wavefunctions, in particular on the energy difference between the target terms that are coupled. It is important therefore to allow for adequate configurating mixing. *IC* collision strengths are finally obtained as

$$\Omega(\Delta_i J_i, \Delta_i' J_i') = \tfrac{1}{2} \sum_{J, j_i} (2J+1) \, | \, T^J(\Delta_i J_i j_i, \Delta_i' J_i' j_{i'}) \, |^2 , \quad (8)$$

where $\Delta_i J_i$ denotes a target fine-structure level, $j_i$ are the partial wave orbitals, and the $T^J$ are transition matrix elements given by

$$\underline{T}^J = -2i\underline{R}^J(\mathbb{1} - i\underline{R}^J)^{-1} . \quad (9)$$

## III. CALCULATIONS

### A. Target representation and data

All states dominated by the configurations $1s^2$, $1s\,2s$, $1s\,2p$, $1s\,3s$, and $1s\,3p$ are included in the scattering problem. These configurations are labeled as principal configurations, as distinct from correlation configurations included to account for CI with the target states. The list for correlation configurations is determined mainly by trial and error, guided by the aim of the best possible values for the eigenenergies of the included states as well as the oscillator strengths for all allowed transitions. Other variables in the atomic structure problem are the adjustable parameters in the Thomas-Fermi-Dirac (TFD) potential that are also so chosen. In our earlier work (PNH) we had the trial configuration list:

$$1s^2, \; 1s\,2s, \; 1s\,2p, \; 1s\,3s, \; 1s\,3p$$

(principal configurations); and

$$2s^2, \; 2p^2, \; 2s\,2p, \; 2p\,3d$$

(correlation configurations). PNH had included the five states, dominated by the first three configurations, in the first term of the eigenstate expansion in Eq. (1a). In the present work we attempted to improve the target representation by also including the configurations $2s\,3s$, $2s\,3p$, $2p\,3s$, and $2p\,3p$, and also by varying the statistical model

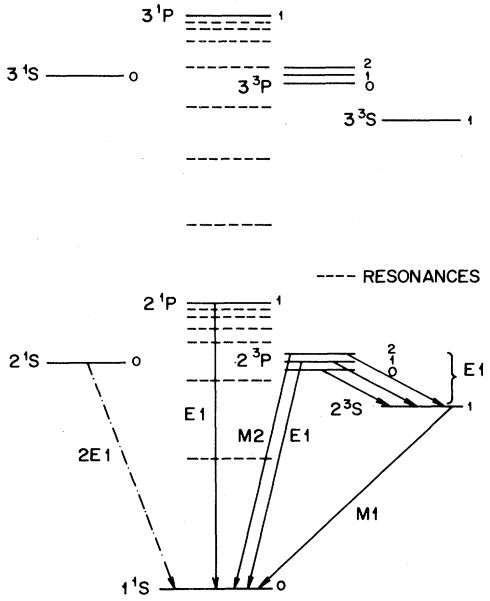


FIG. 1. Energy-level diagram for states considered (not to scale). Dominant modes of radiative decay from the $n = 2$ levels are also shown.

TABLE I. Relativistic eigenenergies for the target states of $Fe^{24+}$, $Se^{32+}$, and $Mo^{40+}$ (in rydbergs).

| State | $Fe^{24+}$ | | $Se^{32+}$ | | $Mo^{40+}$ | |
|---|---|---|---|---|---|---|
| | Present work | EJ | Present work | EJ | Present work | EJ |
| $1^1S_0$ | 0.0 | 0.0 | 0.0 | 0.0 | 0.0 | 0.0 |
| $2^3S_1$ | 488.5291 | 487.8453 | 849.5337 | 847.9665 | 1314.9980 | 1311.8742 |
| $2^3P_0$ | 490.3875 | 489.9809 | 851.9375 | 851.0053 | 1317.7310 | 1316.0274 |
| $2^3P_1$ | 490.6609 | 490.1299 | 852.4595 | 851.2150 | 1318.4893 | 1316.1689 |
| $2^3P_2$ | 491.7766 | 491.1875 | 856.1118 | 854.7431 | 1327.6533 | 1325.0399 |
| $2^1S_0$ | 490.5808 | 490.1502 | 852.1914 | 851.1749 | 1318.2266 | 1316.1115 |
| $2^1P_1$ | 493.1257 | 492.5206 | 857.7520 | 856.3946 | 1329.5854 | 1327.0342 |
| $3^3S_1$ | 578.7344 | 577.9942 | 1007.2354 | 1005.5216 | 1560.5215 | 1556.9685 |
| $3^3P_0$ | 579.2632 | 578.5836 | 1007.9424 | 1006.3593 | 1561.4131 | 1558.1111 |
| $3^3P_1$ | 579.3359 | 578.6237 | 1008.0767 | 1006.4094 | 1561.5942 | 1558.1316 |
| $3^3P_2$ | 579.6528 | 578.9420 | 1009.0947 | 1007.4683 | 1564.0830 | 1560.7829 |
| $3^1S_0$ | 579.2944 | 578.6027 | 1007.9912 | 1006.3692 | 1561.5601 | 1558.0892 |
| $3^1P_1$ | 580.0112 | 579.3052 | 1009.5313 | 1007.9277 | 1564.5933 | 1561.3545 |

potential parameters $\lambda_l$ ($l=s,p,d$) in the TFD potential $V(\lambda_l,r)$. However, it was found that the resulting change in the atomic parameters was not significant (mainly due to the very highly ionized nature of the ions under consideration). It was therefore decided to retain the eigenfunction expansion as in the earlier work with the same associated $\lambda_l$.

In Fig. 1 we show the level structure for all states in-

TABLE II. Relativistic oscillator strengths for allowed transitions in $Fe^{24+}$, $Se^{32+}$, and $Mo^{40+}$. The notation 3.58(−4) is shorthand for $3.58\times10^{-4}$.

| Transition | $Fe^{24+}$ | | | | $Se^{32+}$ | | $Mo^{40+}$ | |
|---|---|---|---|---|---|---|---|---|
| | $S_P$[a] | $S_{SC}$ | $f_P$ | $f_{NBS}$[b] | $S_P$ | $f_P$ | $S_P$ | $f_P$ |
| $1^1S_0$-$2^3P_1$ | 3.58(−4) | | 5.85(−2) | 6.87(−2)[c] | 4.40(−4) | 1.25(−1) | 3.87(−4) | 1.70(−1) |
| $1^1S_0$-$2^1P_1$ | 4.33(−3) | | 7.11(−1) | 7.03(−1)[c] | 2.21(−3) | 6.31(−1) | 1.28(−3) | 5.66(−1) |
| $1^1S_0$-$3^3P_1$ | 5.80(−5) | | 1.12(−2) | 1.70(−2) | 6.30(−5) | 2.11(−2) | 4.90(−5) | 2.54(−2) |
| $1^1S_0$-$3^1P_1$ | 6.82(−4) | | 1.32(−1) | 1.38(−1) | 3.29(−4) | 1.11(−1) | 1.79(−4) | 9.32(−2) |
| $2^3S_1$-$2^3P_0$ | 1.41(−2) | 1.43(−2) | 3.35(−3) | 3.50(−3) | 8.02(−3) | 2.71(−3) | 5.15(−3) | 2.38(−3) |
| $2^3S_1$-$2^3P_1$ | 3.91(−2) | 3.95(−2) | 9.93(−3) | 1.03(−2) | 2.02(−2) | 7.29(−3) | 1.19(−2) | 5.68(−3) |
| $2^3S_1$-$2^3P_2$ | 7.09(−2) | 7.15(−2) | 2.63(−2) | 2.73(−2) | 4.07(−2) | 3.06(−2) | 2.63(−2) | 3.85(−2) |
| $2^3S_1$-$2^1P_1$ | 3.24(−3) | 3.29(−3) | 1.68(−3) | 2.00(−3) | 4.03(−3) | 3.77(−3) | 3.63(−3) | 6.11(−3) |
| $2^3S_1$-$3^3P_0$ | 4.21(−3) | | 4.24(−2) | | 2.38(−3) | 4.19(−2) | 1.48(−3) | 4.05(−2) |
| $2^3S_1$-$3^3P_1$ | 1.15(−2) | | 1.16(−1) | 1.22(−1) | 5.86(−3) | 1.03(−1) | 3.38(−3) | 9.25(−2) |
| $2^3S_1$-$3^3P_2$ | 2.05(−2) | | 2.07(−1) | | 1.13(−2) | 2.00(−1) | 6.86(−3) | 1.90(−1) |
| $2^3S_1$-$3^1P_1$ | 9.93(−4) | | 1.01(−2) | | 1.16(−3) | 2.06(−2) | 9.59(−4) | 2.66(−2) |
| $2^3S_1$-$3^3S_1$ | 4.13(−4) | | 1.21(−2) | | 2.06(−4) | 1.06(−2) | 1.10(−4) | 8.84(−3) |
| $2^3P_1$-$2^1S_0$ | 3.18(−3) | 3.29(−3) | 7.17(−6) | | 3.94(−3) | 5.27−5) | 3.54(−3) | 6.77(−5) |
| $2^3P_1$-$3^3S_1$ | 1.20(−3) | | 1.17(−2) | 1.40(−2) | 5.43(−4) | 9.31(−3) | 2.68(−4) | 7.17(−3) |
| $2^3P_1$-$3^1S_0$ | 8.30(−5) | | 8.16(−4) | | 9.10(−5) | 1.57(−3) | 6.70(−5) | 1.80(−3) |
| $2^3P_2$-$3^3S_1$ | 2.56(−3) | | 1.48(−2) | | 1.50(−3) | 1.51(−2) | 9.97(−4) | 1.54(−2) |
| $2^1S_0$-$2^1P_1$ | 3.95(−2) | 3.95(−2) | 3.12(−2) | 3.29(−2) | 2.05(−2) | 3.57(−2) | 1.22(−2) | 4.44(−2) |
| $2^1S_0$-$3^3P_1$ | 1.16(−3) | | 3.42(−2) | | 1.33(−3) | 6.88(−2) | 1.11(−3) | 8.95(−2) |
| $2^1S_0$-$3^1P_1$ | 1.22(−2) | | 3.63(−1) | 3.64(−1) | 5.97(−3) | 3.12(−1) | 3.32(−3) | 2.71(−1) |
| $2^1P_1$-$3^3S_1$ | 1.41(−4) | | 1.34(−3) | | 1.69(−4) | 2.80(−3) | 1.52(−4) | 3.88(−3) |
| $2^1P_1$-$3^1S_0$ | 1.51(−3) | | 1.44(−2) | 1.40(−2) | 7.63(−4) | 1.27(−2) | 4.50(−4) | 1.16(−2) |
| $3^3S_1$-$3^3P_0$ | 8.70(−2) | | 5.70(−3) | | 5.01(−2) | 4.66(−3) | 3.27(−2) | 4.15(−3) |
| $3^3S_1$-$3^3P_1$ | 2.39(−1) | | 1.67(−2) | 1.60(−2) | 1.24(−1) | 1.22(−2) | 7.48(−2) | 9.67(−3) |
| $3^3S_1$-$3^3P_2$ | 4.34(−1) | | 4.57(−2) | | 2.50(−1) | 5.41(−2) | 1.63(−1) | 6.91(−2) |
| $3^3S_1$-$3^1P_1$ | 2.16(−2) | | 3.15(−3) | | 2.60(−2) | 6.95(−3) | 2.31(−2) | 1.13(−2) |
| $3^1S_0$-$3^3P_1$ | 2.16(−2) | | 1.51(−4) | | 2.60(−2) | 3.48(−4) | 2.31(−2) | 3.26(−4) |
| $3^1S_0$-$3^1P_1$ | 2.37(−1) | | 5.55(−2) | 5.60(−2) | 1.24(−1) | 6.44(−2) | 7.44(−2) | 8.10(−2) |

[a] $S$ refers to the line strengths and the $f$ to oscillator strengths. $P$ is the present work and SC is Sampson and Clark (Ref. 14).
[b] NBS refers to the compilation by Wiese (private communication).
[c] Drake (Ref. 15).

TABLE III. Channels in the pair-coupling scheme: $Mo^{40+}$, $J=2.5$, $\pi$ odd. The channel list refers to $l \leq 4$. The $E_i$ are ion energies in $LS$ coupling.

| Index | $(2S_i+1)_{L_i}$ | $J_i$ | $l_i$ | $K_i$ | $E_i$ (Ry) |
|---|---|---|---|---|---|
| 1 | $^1S$ | 0 | 3 | 3 | 0.0 |
| 2 | $^3S$ | 1 | 1 | 2 | 1286.504 |
| 3 | $^3S$ | 1 | 3 | 2 | 1286.504 |
| 4 | $^3S$ | 1 | 3 | 3 | 1286.504 |
| 5 | $^3P$ | 0 | 2 | 2 | 1289.612 |
| 6 | $^3P$ | 1 | 2 | 2 | 1289.612 |
| 7 | $^3P$ | 1 | 2 | 3 | 1289.612 |
| 8 | $^3P$ | 1 | 4 | 3 | 1289.612 |
| 9 | $^3P$ | 2 | 0 | 2 | 1289.612 |
| 10 | $^3P$ | 2 | 2 | 2 | 1289.612 |
| 11 | $^3P$ | 2 | 2 | 3 | 1289.612 |
| 12 | $^3P$ | 2 | 4 | 2 | 1289.612 |
| 13 | $^3P$ | 2 | 4 | 3 | 1289.612 |
| 14 | $^1S$ | 0 | 3 | 3 | 1290.041 |
| 15 | $^1P$ | 1 | 2 | 2 | 1292.337 |
| 16 | $^1P$ | 1 | 2 | 3 | 1292.337 |
| 17 | $^1P$ | 1 | 4 | 3 | 1292.337 |
| 18 | $^3S$ | 1 | 1 | 2 | 1523.639 |
| 19 | $^3S$ | 1 | 3 | 2 | 1523.639 |
| 20 | $^3S$ | 1 | 3 | 3 | 1523.639 |
| 21 | $^3P$ | 0 | 2 | 2 | 1524.509 |
| 22 | $^3P$ | 1 | 2 | 2 | 1524.509 |
| 23 | $^3P$ | 1 | 2 | 3 | 1524.509 |
| 24 | $^3P$ | 1 | 4 | 3 | 1524.509 |
| 25 | $^3P$ | 2 | 0 | 2 | 1524.509 |
| 26 | $^3P$ | 2 | 2 | 2 | 1524.509 |
| 27 | $^3P$ | 2 | 2 | 3 | 1524.509 |
| 28 | $^3P$ | 2 | 4 | 2 | 1524.509 |
| 29 | $^3P$ | 2 | 4 | 3 | 1524.509 |
| 30 | $^1S$ | 0 | 3 | 3 | 1524.584 |
| 31 | $^1P$ | 1 | 2 | 2 | 1525.241 |
| 32 | $^1P$ | 1 | 2 | 3 | 1525.241 |
| 33 | $^1P$ | 1 | 2 | 3 | 1525.241 |

cluded, along with dominant modes of radiative decay from the $n=2$ levels. The resonances lying between the various complexes are also indicated. In Table I we give the calculated relativistic energy separations relative to the ground state for $Fe^{24+}$, $Se^{32+}$, and $Mo^{40+}$. Values are compared with earlier calculations of Ermolaev and Jones[13] (EJ) who used a different set of target configurations and parameters $\lambda_l$. The EJ calculations were designed specifically to calculate the eigenenergies of He-like ions with a high degree of accuracy and are more accurate than the present values which derive from calculations meant for scattering work, involving a large number of transitions. All of the present energies are in the correct order except for the $2^1S_0$ state in $Fe^{24+}$, which should lie between the $2^3P_1$ and $2^3P_2$ but is seen to be slightly below the $2^3P_1$. There are significant differences between the two sets of calculations, in the energies in a few cases, which manifest themselves in the collision strengths for partial waves $l>15$, where the CB approximation is employed to calculate the contribution to allowed transitions. On the other hand, the dipole line strengths computed in the present work are seen to be fairly accurate. In Table II we give the line and the oscillator strengths for all allowed transitions considered in this work. For $Fe^{24+}$, the line strengths are compared with the calculations of Sampson and Clark[14] and good agreement is found. The oscillator strengths $f_p$ are calculated from the present line strengths *and* the more accurate energy differences given by EJ, using the relation

$$f_{i,j}=\frac{\Delta E_{ij} S_{ij}}{3g_i} .$$

The oscillator strengths for $Fe^{24+}$ are compared with the recent compilation (referred to as NBS) by Wiese (private communication). It is seen that $f$ values for all transitions compared are in good agreement except for the $1^1S_0$-$2^3P_1$. The NBS values for this transition, and the $1^1S_0$-$2^1P_1$, are

TABLE IV. $Z^2$ times the total collision strengths for $(e+Fe^{24+})$.

| Transition | Energy (Ry)/$Z^2$ 0.858 | 1.183 | 1.479 | 2.959 | 7.396 |
|---|---|---|---|---|---|
| $1^1S_1$-$2^3S_1$ | 1.94(−1) | 1.33(−1) | 1.00(−1) | 3.58(−2) | 7.44(−3) |
| $1S_1$-$2^3P_0$ | 1.20(−1) | 7.03(−2) | 4.73(−2) | 1.22(−2) | 2.03(−3) |
| $1^1S_1$-$2^3P_1$ | 4.81(−1) | 4.27(−1) | 4.25(−1) | 5.46(−1) | 8.59(−1) |
| $1^1S_1$-$2^3P_2$ | 5.94(−1) | 3.48(−1) | 2.34(−1) | 6.08(−2) | 8.79(−3) |
| $1^1S_1$-$2^1S_0$ | 5.20(−1) | 6.19(−1) | 6.73(−1) | 7.84(−1) | 8.52(−1) |
| $1^1S_1$-$2^1P_1$ | 1.84(0) | 2.82(0) | 3.58(0) | 6.14(0) | 9.73(0) |
| $1^1S_1$-$3^3S_1$ | 5.68(−2) | 3.85(−2) | 2.84(−2) | 9.46(−3) | 2.03(−3) |
| $1^1S_1$-$3^3P_0$ | 3.65(−2) | 2.16(−2) | 1.42(−2) | 3.38(−3) | 6.76(−4) |
| $1^1S_1$-$3^3P_1$ | 1.24(−1) | 9.87(−2) | 9.06(−2) | 1.01(−1) | 1.61(−1) |
| $1^1S_1$-$3^3P_2$ | 1.89(−1) | 1.12(−1) | 7.30(−2) | 1.83(−2) | 2.70(−3) |
| $1^1S_1$-$3^1S_0$ | 8.38(−2) | 1.14(−1) | 1.28(−1) | 1.57(−1) | 1.74(−1) |
| $1^1S_1$-$3^1P_1$ | 2.80(−1) | 4.60(−1) | 6.06(−1) | 1.08(0) | 1.70(0) |
| $2^3S_1$-$2^3P_0$ | 8.58(1) | 1.10(2) | 1.20(2) | 1.39(2) | 1.58(2) |
| $2^3S_1$-$2^3P_1$ | 2.33(2) | 2.99(2) | 3.23(2) | 3.76(2) | 4.28(2) |
| $2^3S_1$-$2^3P_2$ | 3.71(2) | 4.90(2) | 5.36(2) | 6.31(2) | 7.23(2) |
| $2^3S_1$-$2^1S_0$ | 1.18(0) | 7.17(−1) | 5.57(−1) | 2.12(−1) | 4.53(−2) |
| $2^3S_1$-$2^1P_1$ | 1.74(1) | 2.28(1) | 2.51(1) | 3.01(1) | 3.54(1) |
| $2^3S_1$-$3^3S_1$ | 1.07(1) | 1.35(1) | 1.40(1) | 1.44(1) | 1.26(1) |
| $2^3S_1$-$3^3P_0$ | 1.26(0) | 3.46(0) | 4.70(0) | 8.25(1) | 1.47(1) |
| $2^3S_1$-$3^3P_1$ | 3.50(0) | 9.46(1) | 1.30(1) | 2.35(1) | 4.20(1) |
| $2^3S_1$-$3^3P_2$ | 6.18(0) | 1.68(1) | 2.28(1) | 4.01(1) | 7.10(1) |
| $2^3S_1$-$3^1S_0$ | 3.18(−1) | 5.95(−2) | 2.64(−2) | 3.38(−3) | 6.76(−4) |
| $2^3S_1$-$3^1P_1$ | 1.04(0) | 9.53(−1) | 1.16(0) | 1.95(0) | 3.45(0) |
| $2^3P_0$-$2^3P_1$ | 3.69(0) | 1.78(0) | 1.19(0) | 3.50(−1) | 6.62(−2) |
| $2^3P_0$-$2^3P_2$ | 4.95(0) | 4.50(0) | 4.39(0) | 3.86(0) | 2.58(0) |
| $2^3P_0$-$2^1S_0$ | 1.86(−1) | 5.95(−2) | 3.11(−2) | 5.41(−3) | 6.76(−4) |
| $2^3P_0$-$2^1P_1$ | 1.32(0) | 3.87(−1) | 1.99(−1) | 3.92(−2) | 6.08(−3) |
| $2^3P_0$-$3^3S_1$ | 2.31(−1) | 3.62(−1) | 4.89(−1) | 8.92(−1) | 1.62(0) |
| $2^3P_0$-$3^3P_0$ | 3.47(0) | 4.27(0) | 4.41(0) | 4.51(0) | 4.16(0) |
| $2^3P_0$-$3^3P_1$ | 4.50(−1) | 8.86(−1) | 3.79(−2) | 4.73(−3) | 6.76(−4) |
| $2^3P_0$-$3^3P_2$ | 8.45(−1) | 6.96(−1) | 6.20(−1) | 3.11(−1) | 1.57(−1) |
| $2^3P_0$-$3^1S_0$ | 6.69(−2) | 1.55(−2) | 6.76(−3) | 6.76(−4) | 0.00(0) |
| $2^3P_0$-$3^1P_1$ | 4.85(−1) | 9.73(−2) | 4.19(−2) | 5.41(−3) | 6.76(−4) |
| $2^3P_1$-$2^3P_2$ | 1.46(1) | 1.10(1) | 1.01(1) | 8.25(0) | 5.41(0) |
| $2^3P_1$-$2^1S_0$ | 4.56(2) | 5.06(2) | 5.27(1) | 5.66(1) | 6.06(1) |
| $2^3P_1$-$2^2P_1$ | 5.18(0) | 3.04(0) | 2.59(0) | 1.95(0) | 1.24(0) |
| $2^3P_1$-$3^3S_1$ | 6.89(−1) | 1.03(0) | 1.39(0) | 2.55(0) | 4.68(0) |
| $2^3P_1$-$3^3P_0$ | 4.47(−1) | 8.79(−2) | 3.72(−2) | 4.73(−2) | 6.76(−4) |
| $2^3P_1$-$3^3P_1$ | 1.14(1) | 1.34(1) | 1.37(1) | 1.39(1) | 1.27(1)* |
| $2^3P_1$-$S^3P_2$ | 2.55(0) | 1.63(0) | 1.38(0) | 6.66(−1) | 3.32(−1) |
| $2^3P_1$-$3^1S_0$ | 2.12(−1) | 1.21(−1) | 1.28(−1) | 1.95(−1) | 3.38(−1) |
| $2^3P_1$-$3^1P_1$ | 1.45(0) | 5.52(−1) | 3.93(−1) | 1.62(−1) | 7.91(−2) |
| $2^3P_2$-$2^1S_0$ | 9.26(−1) | 2.96(−1) | 1.55(−1) | 2.64(−2) | 3.38(−3) |
| $2^3P_2$-$2^1P_1$ | 7.77(0) | 3.70(0) | 2.68(0) | 1.25(0) | 5.58(−1) |
| $2^3P_2$-$3^3S_1$ | 1.21(0) | 1.99(0) | 2.72(0) | 5.22(0) | 9.80(0) |

computed by Drake[15] who has developed an improved, unified relativistic theory for these transitions, yielding more accurate values than the method of Eissner *et al.* The available NBS values are used in the CB calculations for $Fe^{24+}$, together with Drake's values for the two transitions mentioned [1.44(−1) and 6.23(−1), respectively, for $Se^{32+}$ and 1.95(−1), and 5.61(−1) for $Mo^{40+}$]. Lin, Johnson, and Dalgarno[16] have also computed oscillator strengths for the transitions $2^3S_1-2^3P_{0,1,2}$ in $Fe^{24+}$ and $Mo^{40+}$. Their values are 3.30(−3), 9.70(−3), and 2.82(−2), respectively, for $Fe^{24+}$ and 2.30(−3), 5.30(−3), and 3.94(−2) for $Mo^{40+}$, and compare well with those in Table II. The oscillator strengths given in Table II differ from the ones calculated with present energies only slightly in most cases; however, in some instances the differences are considerable. For example, the present values for the transitions $2^3S_1$-$2^3P_{0,1}$ in $Mo^{40+}$ are 1.60(−3) and 4.60(−3), respectively, and are much lower than the form-

TABLE IV. (*Continued.*)

| Transition | Energy (Ry)/$Z^2$ 0.858 | 1.183 | 1.479 | 2.959 | 7.396 |
|---|---|---|---|---|---|
| $2^3P_2$-$3^3P_0$ | 8.31(−1) | 7.37(−1) | 6.64(−1) | 3.43(−1) | 1.72(−1) |
| $2^3P_2$-$3^3P_1$ | 2.49(0) | 1.68(0) | 1.44(0) | 7.17(−1) | 3.54(−1) |
| $2^3P_2$-$3^3P_2$ | 2.22(1) | 2.46(1) | 2.49(1) | 2.47(1) | 2.24(1) |
| $2^3P_2$-$3^1S_0$ | 3.33(−1) | 7.84(−2) | 3.52(−2) | 4.73(−3) | 6.76(−4) |
| $2^3P_2$-$3^1P_1$ | 2.19(0) | 5.28(−1) | 2.87(−1) | 8.11(−2) | 3.31(−2) |
| $2^1S_0$-$2^1P_1$ | 2.29(0) | 3.00(2) | 3.27(2) | 3.81(2) | 4.35(2) |
| $2^1S_0$-$S^3S_1$ | 3.24(−1) | 6.42(−2) | 2.97(−2) | 4.73(−3) | 6.76(−4) |
| $2^1S_0$-$3^3P_0$ | 8.79(−2) | 1.69(−2) | 7.44(−3) | 6.76(−4) | |
| $2^1S_0$-$3^3P_1$ | 5.48(−1) | 9.87(−1) | 1.32(0) | 2.31(0) | 4.10(0) |
| $2^1S_0$-$3^3P_2$ | 4.63(−1) | 8.59(−2) | 3.58(−2) | 4.06(−3) | |
| $2^1S_0$-$3^1S_0$ | 4.24(0) | 5.44(0) | 5.67(0) | 5.82(0) | 5.02(0) |
| $2^1S_0$-$3^1P_1$ | 3.10(0) | 9.87(0) | 1.36(1) | 2.41(1) | 4.30(1) |
| $2^1P_1$-$3^3S_1$ | 6.16(−1) | 2.27(−1) | 1.95(−1) | 2.85(−1) | 5.35(−1) |
| $2^1P_1$-$3^3P_0$ | 4.61(−1) | 9.33(−2) | 4.06(−2) | 5.41(−3) | 6.76(−4) |
| $2^1P_1$-$3^3P_1$ | 1.41(0) | 5.88(−1) | 4.41(−1) | 1.96(−1) | 9.53(−2) |
| $2^1P_1$-$3^3P_2$ | 2.18(0) | 5.21(−1) | 2.83(−1) | 8.11(−2) | 3.24(−2) |
| $2^1P_1$-$3^1S_0$ | 3.45(−1) | 1.11(0) | 1.58(0) | 3.06(0) | 5.69(0) |
| $2^1P_1$-$3^1P_1$ | 1.35(1) | 1.64(1) | 1.67(1) | 1.62(1) | 1.45(1) |
| $3^3S_1$-$3^3P_0$ | 2.92(2) | 7.23(2) | 7.91(2) | 9.26(2) | 1.09(3) |
| $3^3S_1$-$3^3P_1$ | 7.71(2) | 1.88(3) | 2.06(3) | 2.41(3) | 2.84(3) |
| $3^3S_1$-$3^3P_2$ | 1.22(3) | 3.22(3) | 3.66(3) | 4.25(3) | 5.06(3) |
| $3^3S_1$-$3^1S_0$ | 2.27(0) | 9.87(−1) | 7.64(−1) | 2.71(−1) | 5.48(−2) |
| $3^3S_1$-$3^1P_1$ | 5.78(1) | 1.47(2) | 1.62(2) | 1.96(2) | 2.36(2) |
| $3^3P_0$-$3^3P_1$ | 4.64(0) | 1.45(0) | 9.73(−1) | 2.97(−1) | 5.68(−2) |
| $3^3P_0$-$3^3P_2$ | 3.78(1) | 2.83(1) | 2.33(1) | 1.18(1) | 5.28(0) |
| $3^3P_0$-$3^1S_0$ | 3.90(−1) | 3.04(−2) | 1.15(−2) | 6.76(−4) | |
| $3^3P_0$-$3^1P_1$ | 2.24(0) | 2.07(−1) | 1.07(−1) | 2.64(−2) | 4.73(−3) |
| $3^3P_1$-$3^3P_2$ | 8.45(1) | 5.92(1) | 4.85(1) | 2.44(1) | 1.09(1) |
| $3^3P_1$-$3^1S_0$ | 1.45(2) | 3.06(2) | 3.22(2) | 3.57(2) | 3.97(2) |
| $3^3P_1$-$3^1P_1$ | 2.39(1) | 1.51(1) | 1.23(1) | 6.14(0) | 2.72(0) |
| $3^3P_2$-$3^1S_0$ | 1.95(0) | 1.51(−1) | 5.68(−2) | 2.70(−3) | |
| $3^3P_2$-$3^1P_1$ | 1.71(1) | 7.98(0) | 6.27(0) | 2.83(0) | 1.11(0) |
| $3^1S_0$-$3^1P_1$ | 6.83(2) | 1.90(3) | 2.08(3) | 2.47(3) | 2.92(3) |

er corresponding values in Table II. Similar differences are also found for the transition $3^3S_1$-$3^3P_0$ in $Se^{32+}$ and $Mo^{40+}$, and for transitions $2^3P_1$-$2^1S_0$ and $3^3P_1$-$3^1S_0$ in all three ions. In the CB calculations (Sec. III B 3), the oscillator strengths $f_p$ in Table II are used along with the energies given by EJ.

### B. Collision strengths

As noted earlier we carried out rather extensive nine-state calculations in both the CC and the DW approximations in order to determine whether any significant differences were present in, for example, low partial waves or at energies very near the excitation thresholds. Detailed examination of the reactance matrices $\underline{R}^{DW}$ and $\underline{R}^{CC}$ revealed, in general, no more than a few percent discrepancies and the collision strengths in both approximations were therefore in the same range of accuracy. In view of the close agreement it is not felt necessary to give a detailed comparison. We employed the $\underline{R}^{DW}$ for the first fifteen partial waves in computing the nonresonant collision strengths given in this paper, and the $\underline{R}^{CC}$ for the first five partial waves for resonance analysis in paper II. Basic features of the two sets of scattering calculations are described below.

#### 1. Close coupling

Coupling the partial waves $l$, $l' \leq 4$ of the colliding electron with the nine $L_iS_i$ states dominated by the principal configurations results in the following ten states with total ($e$ plus ion) spin multiplicity $(2S+1)$, orbital angular momentum $L$, and parity $\pi$, i.e., $^{2S+1}L^{\pi}$:

$$^{(4,2)}(S,D,G,P^o,F^o)\ ,$$

which connect transitions between different $L_iS_i$ states of the target. In addition, for transitions involving the fine-structure states $n^3P^o_J$, one needs the states

$$^{(4,2)}[P,F,D^o,G^o,H^o]$$

TABLE V. $Z^2$ times the total collision strengths for $(e+Se^{32+})$.

| Transition | Energy (Ry)/$Z^2$ 0.8737 | 1.2976 | 1.7301 | 4.3253 | 8.6505 |
|---|---|---|---|---|---|
| $1^1S_1$-$2^3S_1$ | 1.91(−1) | 1.17(−1) | 7.86(−2) | 1.85(−2) | 5.78(−3) |
| $1^1S_1$-$2^3P_0$ | 1.20(−1) | 6.13(−2) | 3.58(−2) | 5.78(−3) | 1.16(−3) |
| $1^1S_1$-$2^3P_1$ | 6.30(−1) | 6.99(−1) | 8.12(−1) | 1.38(0) | 1.93(0) |
| $1^1S_1$-$2^3P_2$ | 5.92(−1) | 2.99(−1) | 1.77(−1) | 2.89(−2) | 6.94(−3) |
| $1^1S_1$-$2^1S_0$ | 5.25(−1) | 6.40(−1) | 7.02(−1) | 8.18(−1) | 8.58(−1) |
| $1^1S_1$-$2^1P_1$ | 1.71(0) | 2.79(0) | 3.66(0) | 6.72(0) | 9.06(0) |
| $1^1S_1$-$3^3S_1$ | 5.55(−2) | 3.24(−2) | 2.20(−2) | 4.62(−3) | 1.16(−3) |
| $1^1S_1$-$3^3P_0$ | 3.70(−2) | 1.85(−2) | 1.04(−2) | 1.16(−3) | |
| $1^1S_1$-$3^3P_1$ | 1.48(−1) | 1.35(−1) | 1.48(−1) | 2.32(−1) | 2.98(−1) |
| $1^1S_1$-$3^3P_2$ | 1.94(−1) | 9.48(−2) | 5.43(−2) | 8.09(−3) | 2.31(−3) |
| $1^1S_1$-$3^1S_0$ | 8.55(−2) | 1.19(−1) | 1.34(−1) | 1.64(−1) | 1.73(−1) |
| $1^1S_1$-$3^1P_1$ | 3.05(−1) | 4.75(−1) | 6.38(−1) | 1.18(0) | 1.54(0) |
| $2^3S_1$-$2^3P_0$ | 8.63(1) | 1.12(2) | 1.21(2) | 1.41(2) | 1.55(2) |
| $2^3S_1$-$2^3P_1$ | 2.13(2) | 2.77(2) | 3.01(2) | 3.51(2) | 3.84(2) |
| $2^3S_1$-$2^3P_2$ | 3.36(2) | 4.64(2) | 5.13(2) | 6.15(2) | 6.81(2) |
| $2^3S_1$-$2^1S_0$ | 1.17(0) | 6.50(−1) | 4.54(−1) | 1.14(−1) | 3.35(−2) |
| $2^3S_1$-$2^1P_1$ | 3.20(1) | 4.36(1) | 4.82(1) | 5.82(1) | 6.47(1) |
| $2^3S_1$-$3^3S_1$ | 9.98(0) | 1.27(1) | 1.32(1) | 1.33(1) | 1.13(1) |
| $2^3S_1$-$3^3P_0$ | 1.30(0) | 3.89(0) | 5.34(0) | 1.02(1) | 1.52(1) |
| $2^3S_1$-$3^3P_1$ | 3.34(0) | 9.60(0) | 1.32(1) | 2.52(1) | 3.75(1) |
| $2^3S_1$-$3^3P_2$ | 6.27(0) | 1.85(1) | 2.54(1) | 4.84(1) | 7.21(1) |
| $2^3S_1$-$3^1S_0$ | 3.19(−1) | 4.16(−2) | 1.62(−2) | 1.16(−3) | |
| $2^3S_1$-$3^1P_1$ | 1.32(0) | 1.98(0) | 2.62(0) | 4.92(0) | 7.34(0) |
| $2^3P_0$-$2^3P_1$ | 3.54(0) | 1.51(0) | 9.04(−1) | 1.83(−1) | 5.09(−2) |
| $2^3P_0$-$2^3P_2$ | 4.88(0) | 4.38(0) | 4.24(0) | 3.33(0) | 2.34(0) |
| $2^3P_0$-$2^1S_0$ | 1.83(−1) | 4.62(−2) | 2.08(−2) | 2.31(−3) | |
| $2^3P_0$-$2^1P_1$ | 1.43(0) | 3.11(−1) | 1.31(−1) | 1.39(−2) | 3.47(−3) |
| $2^3P_0$-$3^3S_1$ | 2.22(−1) | 3.69(−1) | 5.05(−1) | 1.02(0) | 1.49(0) |
| $2^3P_0$-$3^3P_0$ | 3.20(0) | 4.01(0) | 4.13(0) | 4.15(0) | 3.76(0) |
| $2^3P_0$-$3^3P_1$ | 4.32(−1) | 5.78(−2) | 2.08(−2) | 1.16(−3) | |
| $2^3P_0$-$3^3P_2$ | 8.45(−1) | 6.45(−1) | 5.20(−2) | 2.06(−1) | 1.32(−1) |
| $2^3P_0$-$3^1S_0$ | 6.47(−2) | 1.04(−2) | 4.62(−3) | | |
| $2^3P_0$-$3^1P_1$ | 5.01(−1) | 7.17(−2) | 2.66(−2) | 2.31(−3) | |
| $2^3P_1$-$2^3P_2$ | 1.34(1) | 9.40(0) | 8.54(0) | 6.33(0) | 4.42(0) |
| $2^3P_1$-$2^1S_0$ | 9.38(1) | 1.08(2) | 1.12(2) | 1.22(2) | 1.29(2) |
| $2^3P_1$-$2^1P_1$ | 6.43(0) | 4.51(0) | 4.14(0) | 3.12(0) | 2.17(0) |
| $2^3P_1$-$3^3S_1$ | 6.47(−1) | 9.57(−1) | 1.30(0) | 2.65(0) | 3.89(0) |
| $2^3P_1$-$3^3P_0$ | 4.30(−1) | 5.78(−2) | 2.08(−2) | 1.16(−3) | |
| $2^3P_1$-$3^3P_1$ | 1.06(1) | 1.24(1) | 1.27(1) | 1.27(1) | 1.14(1) |
| $2^3P_1$-$3^3P_2$ | 2.57(0) | 1.38(0) | 1.05(0) | 3.99(−1) | 2.53(−1) |
| $2^3P_1$-$3^1S_0$ | 2.17(−1) | 2.05(−1) | 2.59(−1) | 4.77(−1) | 6.79(−1) |
| $2^3P_1$-$3^1P_1$ | 1.51(0) | 7.14(−1) | 5.28(−1) | 1.97(−1) | 1.26(−1) |
| $2^3P_2$-$2^1S_0$ | 9.10(−1) | 2.31(−1) | 1.02(−1) | 1.16(−2) | 2.31(−3) |
| $2^3P_2$-$2^1P_1$ | 8.61(0) | 4.25(0) | 3.16(0) | 1.57(0) | 9.63(−1) |
| $2^3P_2$-$3^3S_1$ | 1.17(0) | 2.19(0) | 3.09(0) | 6.94(0) | 1.05(1) |

in the summation over $SL\pi$ in Eq. (5). Altogether there are twenty total $(2S+1)L\pi$ states and the coupled ID equations of the CC approximation are solved separately for each symmetry to obtain $\underline{R}^{CC}(SL\pi)$. With the target representation as described in Sec. III A, angular integral and radial integral coefficients, describing the $e$ plus ion potential operators, are calculated as discussed by Eissner and Seaton[6] and, using this collisional data, the ID equations are set up and solved by the linear-algebraic method developed by Crees *et al.*[17] Calculations are carried out at the energies of interest (which in the present case are only a few) in the energy range above all thresholds. The largest calculations are for symmetries $^2P^o$ and $^2D$ with thirteen "free channels" in each case, i.e., the terms of the first sum in Eq. (1a), and with 31 and 29 "bound channels" [the second sum in Eq. (1b)], respectively.

### 2. *Distorted wave*

With $l$, $l' \leq 15$ the number of total $SL\pi$ states is much larger than for the CC case. If we write $2L$ for twice the total orbital angular momentum of the $e$ plus ion system, and $(2L)_{max}$ for its maximum value, then the states $^{(2S+1)}(2L,2L_{max},2)$ required for the collision problem are

TABLE V. (*Continued.*)

| Transition | Energy (Ry)/$Z^2$ 0.8737 | 1.2976 | 1.7301 | 4.3253 | 8.6505 |
|---|---|---|---|---|---|
| $2^3P_2$-$3^3P_0$ | 8.21(−1) | 7.11(−1) | 5.92(−1) | 2.45(−1) | 1.54(−1) |
| $2^3P_2$-$3^3P_1$ | 2.45(0) | 1.46(0) | 1.15(0) | 4.58(−1) | 2.86(−1) |
| $2^3P_2$-$3^3P_2$ | 2.20(1) | 2.42(1) | 2.44(1) | 2.37(1) | 2.10(1) |
| $2^3P_2$-$3^1S_0$ | 3.21(−1) | 5.43(−2) | 2.08(−2) | 2.31(−3) | |
| $2^3P_2$-$3^1P_1$ | 2.17(0) | 5.16(−1) | 3.09(−1) | 9.71(−2) | 5.90(−2) |
| $2^1S_0$-$2^1P_1$ | 1.82(2) | 2.50(2) | 2.75(2) | 3.26(2) | 3.61(2) |
| $2^1S_0$-$3^3S_1$ | 3.24(−1) | 4.51(−2) | 1.73(−2) | 1.16(−3) | |
| $2^1S_0$-$3^3P_0$ | 9.02(−2) | 1.16(−2) | 4.62(−3) | | |
| $2^1S_0$-$3^3P_1$ | 8.46(−1) | 2.19(0) | 3.00(0) | 5.76(0) | 8.58(0) |
| $2^1S_0$-$3^3P_2$ | 4.58(−1) | 5.90(−2) | 2.08(−2) | 1.16(−3) | |
| $2^1S_0$-$3^1S_0$ | 4.21(0) | 5.42(0) | 5.60(0) | 5.56(0) | 4.62(0) |
| $2^1S_0$-$3^1P_1$ | 2.85(0) | 9.69(0) | 1.34(1) | 2.58(1) | 3.84(1) |
| $2^1P_1$-$3^3S_1$ | 6.09(−1) | 3.13(−1) | 3.63(−1) | 7.72(−1) | 1.17(0) |
| $2^1P_1$-$3^3P_0$ | 4.64(−1) | 6.70(−2) | 2.54(−2) | 2.31(−3) | |
| $2^1P_1$-$3^3P_1$ | 1.45(0) | 8.03(−1) | 6.27(−1) | 2.50(−1) | 1.56(−1) |
| $2^1P_1$-$3^3P_2$ | 2.16(0) | 5.12(−1) | 3.09(−1) | 9.83(−2) | 5.90(−2) |
| $2^1P_1$-$3^1S_0$ | 3.06(−1) | 1.12(0) | 1.63(0) | 3.64(0) | 5.43(0) |
| $2^1P_1$-$3^1P_1$ | 1.29(1) | 1.55(1) | 1.56(1) | 1.50(1) | 1.33(1) |
| $3^3S_1$-$3^3P_0$ | 3.14(2) | 7.64(2) | 8.36(2) | 1.01(3) | 1.13(3) |
| $3^3S_1$-$3^3P_1$ | 7.63(2) | 1.87(3) | 2.04(3) | 2.47(3) | 2.76(3) |
| $3^3S_1$-$3^3P_2$ | 1.13(3) | 3.18(3) | 3.53(3) | 4.39(3) | 4.98(3) |
| $3^3S_1$-$3^1S_0$ | 2.29(0) | 8.95(−1) | 6.22(−1) | 1.43(−1) | 4.16(−2) |
| $3^3S_1$-$3^1P_1$ | 1.13(2) | 3.13(2) | 3.50(2) | 4.39(2) | 5.00(2) |
| $3^3P_0$-$3^3P_1$ | 4.44(0) | 1.25(0) | 7.77(−1) | 1.61(−1) | 4.51(−2) |
| $3^3P_0$-$3^3P_2$ | 3.73(1) | 2.60(1) | 2.00(1) | 8.38(0) | 4.60(0) |
| $3^3P_0$-$3^1S_0$ | 3.86(−1) | 1.97(−2) | 5.78(−3) | | |
| $3^3P_0$-$3^1P_1$ | 2.45(0) | 1.20(−1) | 4.39(−2) | 4.62(−3) | 1.16(−3) |
| $3^3P_1$-$3^3p_2$ | 7.59(1) | 4.90(1) | 3.73(1) | 1.56(1) | 8.57(0) |
| $3^3P_1$-$3^1S_0$ | 3.10(2) | 6.39(2) | 6.76(2) | 7.66(2) | 8.38(2) |
| $3^3P_1$-$3^1P_1$ | 3.91(1) | 2.53(1) | 1.93(1) | 8.10(0) | 4.45(0) |
| $3^3P_2$-$3^1S_0$ | 1.93(0) | 1.01(−1) | 3.12(−2) | | |
| $3^3P_2$-$3^1P_1$ | 2.43(1) | 1.27(1) | 9.41(0) | 3.62(0) | 1.90(0) |
| $3^1S_0$-$3^1P_1$ | 5.62(2) | 1.66(3) | 1.84(3) | 2.26(3) | 2.55(3) |

$^{(4,2)}[0,32,2]$

for even $\pi$ and

$^{(4,2)}[2,30,21]$

for odd $\pi$ where the $2L$ is incremented in steps of 2 (note that there are no $^{(4,2)}S^o$ states). Thus altogether there are 80 symmetries for the $(N+1)$-electron system to be considered. Calculations are carried out at a small number of energies above the $n=3$ states, up to about ten times the threshold excitation energies. The energy mesh for each ion is chosen so as to bring out some structure that is present in the nonresonant collision strengths (which will be discussed later). In addition, DW calculations are also done at a fairly large number of energies, mainly in the region somewhere above the $n=2$ states, in order to complement the analysis of resonance structures converging on to the $n=3$ states (paper II). The DW calculations are described in our earlier work (PNH) and most of the details concerning the nonresonant calculations remain the same.

### 3. *Coulomb-Bethe*

The contribution to the collision strengths from large $l$ values for optically allowed transitions may be evaluated using the CB approximation which has been rendered in a convenient computational form by Burgess and Sheorey.[18] The partial CB collision strength is expressed as

$$\Omega^l_{\rm CB}(\Delta_i J_i,\Delta_f J_f)=\frac{4}{\sqrt{3}}\frac{g(J_i)f(\Delta_i J_i,\Delta_f J_f)}{[E(\Delta_f J_f)-E(\Delta_i J_i)]}G^l(k,k')\ . \tag{10}$$

where subscripts $i$ and $f$ refer to initial and final levels, $f$ is the absorption oscillator strength, and $G^l(k,k')$ is the free-free Gaunt factor evaluated by Burgess[19,20] in terms of the regular Coulomb functions in a closed form. The applicability of Eq. (10), with particular reference to very highly charged ions where IC effects become prominent, has been discussed in detail by Jones.[12] We take into consideration the points made by Jones and employ the following steps to calculate the high-$l$ contributions: (i)

TABLE VI. $Z^2$ times the total collision strengths for $(e+Mo^{40+})$.

| Transition | Energy (Ry)/$Z^2$ 0.8900 | 1.0200 | 1.1338 | 2.8340 | 8.5030 |
|---|---|---|---|---|---|
| $1^1S_1$-$2^3S_1$ | 1.87(−1) | 1.55(−1) | 1.36(−1) | 3.70(−2) | 5.29(−3) |
| $1^1S_1$-$2^3P_0$ | 1.20(−1) | 9.35(−2) | 7.76(−2) | 1.41(−2) | 1.76(−3) |
| $1^1S_1$-$2^3P_1$ | 7.46(−1) | 7.85(−1) | 8.27(−1) | 1.47(0) | 2.59(0) |
| $1^1S_1$-$2^3P_2$ | 5.84(−4) | 4.57(−1) | 3.83(−1) | 6.88(−2) | 7.06(−3) |
| $1^1S_1$-$2^1S_0$ | 5.31(−1) | 5.77(−1) | 6.17(−1) | 7.74(−1) | 8.56(−1) |
| $1^1S_1$-$2^1P_1$ | 1.63(0) | 1.94(0) | 2.19(0) | 4.71(0) | 8.01(0) |
| $1^1S_1$-$3^3S_1$ | 5.29(−2) | 4.41(−2) | 3.70(−2) | 8.82(−3) | 1.76(−3) |
| $1^1S_1$-$3^3P_0$ | 3.70(−2) | 2.82(−2) | 2.29(−2) | 3.53(−3) | |
| $1^1S_1$-$3^3P_1$ | 1.73(−1) | 1.59(−1) | 1.59(−1) | 2.43(−1) | 3.76(−1) |
| $1^1S_1$-$3^3P_2$ | 1.96(−1) | 1.50(−1) | 1.23(−1) | 1.94(−2) | 1.76(−3) |
| $1^1S_1$-$3^1S_0$ | 8.82(−2) | 1.01(−1) | 1.09(−1) | 1.52(−1) | 1.73(−1) |
| $1^1S_1$-$3^1P_1$ | 3.42(−1) | 3.61(−1) | 3.97(−1) | 8.48(−1) | 1.35(0) |
| $2^3S_1$-$2^3P_0$ | 8.17(1) | 9.95(2) | 1.06(2) | 1.33(2) | 1.54(2) |
| $2^3S_1$-$2^3P_1$ | 2.01(2) | 2.28(2) | 2.42(2) | 3.05(2) | 3.53(2) |
| $2^3S_1$-$2^3P_2$ | 3.05(2) | 3.81(2) | 3.95(2) | 5.36(2) | 6.42(2) |
| $2^3S_1$-$2^1S_0$ | 1.14(0) | 8.77(−1) | 7.62(−1) | 2.26(−1) | 3.53(−2) |
| $2^3S_1$-$2^1P_1$ | 4.09(1) | 4.83(1) | 5.24(1) | 7.15(1) | 8.59(1) |
| $2^3S_1$-$3^3S_1$ | 9.08(0) | 1.06(1) | 1.11(1) | 1.23(1) | 1.05(1) |
| $2^3S_1$-$3^3P_0$ | 1.39(0) | 2.31(0) | 2.99(0) | 7.34(0) | 1.42(1) |
| $2^3S_1$-$3^3P_1$ | 3.35(0) | 5.33(0) | 6.85(0) | 1.68(1) | 3.25(1) |
| $2^3S_1$-$3^3P_2$ | 6.69(0) | 1.07(1) | 1.38(1) | 3.38(1) | 6.56(1) |
| $2^3S_1$-$3^1S_0$ | 2.95(−1) | 1.18(−1) | 7.06(−2) | 3.53(−3) | |
| $2^3S_1$-$3^1P_1$ | 1.52(0) | 1.75(0) | 2.10(0) | 4.73(0) | 9.16(0) |
| $2^3P_0$-$2^3P_1$ | 3.33(0) | 2.36(0) | 1.91(0) | 3.85(−1) | 5.29(−2) |
| $2^3P_0$-$2^3P_2$ | 4.79(0) | 4.50(0) | 4.41(0) | 3.81(0) | 2.35(0) |
| $2^3P_0$-$2^1S_0$ | 1.75(−1) | 1.01(−1) | 7.06(−2) | 5.29(−3) | |
| $2^3P_0$-$2^1P_1$ | 1.47(0) | 8.01(−1) | 5.45(−1) | 4.06(−2) | 3.53(−3) |
| $2^3P_0$-$3^3S_1$ | 2.15(−1) | 2.27(−1) | 2.67(−1) | 6.37(−1) | 1.22(0) |
| $2^3P_0$-$3^3P_0$ | 2.91(0) | 3.35(0) | 3.51(0) | 3.81(0) | 3.48(0) |
| $2^3P_0$-$3^3P_1$ | 3.93(−1) | 1.64(−1) | 9.88(−2) | 5.29(−3) | |
| $2^3P_0$-$3^3P_2$ | 8.36(−1) | 6.88(−1) | 6.58(−1) | 2.86(−1) | 1.24(−1) |
| $2^3P_0$-$3^1S_0$ | 6.00(−2) | 2.82(−2) | 1.76(−2) | 1.76(−3) | |
| $2^3P_0$-$3^1P_1$ | 4.80(−1) | 2.10(−1) | 1.29(−1) | 7.06(−3) | |
| $2^3P_1$-$2^3P_2$ | 1.24(1) | 1.01(1) | 9.30(0) | 6.76(0) | 4.07(0) |
| $2^3P_1$-$2^1S_0$ | 1.30(2) | 1.38(2) | 1.43(2) | 1.63(2) | 1.77(2) |
| $2^3P_1$-$2^1P_1$ | 7.07(0) | 6.10(0) | 5.77(0) | 4.59(0) | 2.80(0) |
| $2^3P_1$-$3^3S_1$ | 6.12(−1) | 6.50(−1) | 6.59(−1) | 1.52(0) | 2.94(0) |
| $2^3P_1$-$2^3P_0$ | 3.92(−1) | 1.64(−1) | 9.88(−2) | 5.29(−3) | |
| $2^3P_1$-$3^3P_1$ | 9.61(0) | 1.06(1) | 1.09(1) | 1.16(1) | 1.06(1) |
| $2^3P_1$-$3^3P_2$ | 2.49(0) | 1.65(0) | 1.43(0) | 5.17(−1) | 2.19(−1) |
| $2^3P_1$-$3^1S_0$ | 2.19(−1) | 1.96(−1) | 2.13(−1) | 4.30(−1) | 7.74(−1) |
| $2^3P_1$-$3^1P_1$ | 1.50(0) | 1.05(0) | 9.30(−1) | 3.49(−1) | 1.50(−1) |
| $2^3P_2$-$2^1S_0$ | 8.64(−1) | 5.01(−1) | 3.51(−1) | 3.00(−2) | 1.76(−3) |
| $2^3P_2$-$2^1P_1$ | 8.98(0) | 6.72(0) | 5.77(0) | 2.70(0) | 1.32(0) |
| $2^3P_2$-$3^3S_1$ | 1.12(0) | 1.39(0) | 1.70(0) | 4.86(0) | 1.05(1) |

determine a sufficiently high-$l$ value beyond which to activate the CB approximation (see below), (ii) use relativistic dipole oscillator strengths in Eq. (10), and (iii) use relativistic energy separations. This approach should yield a fairly accurate summation over the partial waves $l > l_{\max}$, where, following Seaton,[21]

$$l_{\max} \simeq (k^2\bar{r}^2 + 2z\bar{r} + \tfrac{1}{4})^{1/2} - \tfrac{1}{2} , \tag{11}$$

and where we take $\bar{r}$ to be the mean expectation value of $r$ for the farthermost orbital in the target ion; $k^2$ is the incident kinetic energy and $z$ is the ion change. Furthermore, in order that $\Omega^l$ be independent of the uncertainty in the transition energy $\Delta E$, one must have

$$l\,\Delta E \ll k_i^2 , \tag{12}$$

where $k_i^2$ is the energy relative to the initial level.

For the three ions under study, $Fe^{24+}$, $Se^{32+}$, and $Mo^{40+}$, $\bar{r} = \bar{r}(3p)$ since the $3p$ orbital is the most extended one (more than the $3d$, which is for correlation purpose only). In the TFD potential $V(\lambda_l, r)$ we choose $\lambda_p \simeq 0.836$, and $\lambda_d = 1.0$ for all three ions. We obtain $\bar{r}(\mathrm{Fe}) = 0.50$, $\bar{r}(\mathrm{Se}) = 0.38$, and $\bar{r}(\mathrm{Mo}) = 0.30$. For $k^2$ up to at least five

TABLE VI. (*Continued.*)

| Transition | Energy (Ry)/$Z^2$ 0.8900 | 1.0200 | 1.1338 | 2.8340 | 8.5030 |
|---|---|---|---|---|---|
| $2^3P_2$-$3^3P_0$ | 8.00(−1) | 7.29(−1) | 7.29(−1) | 3.67(−1) | 1.57(−1) |
| $2^3P_2$-$3^3P_1$ | 2.31(0) | 1.67(0) | 1.51(0) | 6.40(−1) | 2.68(−1) |
| $2^3P_2$-$3^3P_2$ | 2.15(1) | 2.28(1) | 2.33(1) | 2.35(1) | 2.06(1) |
| $2^3P_2$-$3^1S_0$ | 2.95(−1) | 1.41(−1) | 9.00(−2) | 5.29(−3) | |
| $2^3P_2$-$3^1P_1$ | 2.05(0) | 1.07(0) | 7.89(−1) | 1.99(−1) | 7.94(−2) |
| $2^1S_0$-$2^1P_1$ | 1.49(2) | 1.78(2) | 1.93(2) | 2.60(2) | 3.08(2) |
| $2^1S_3$-$3^3S_1$ | 2.98(−1) | 1.22(−1) | 7.41(−2) | 5.29(−3) | |
| $2^1S_0$-$3^3P_0$ | 8.29(−2) | 3.53(−2) | 2.12(−2) | 1.76(−3) | |
| $2^1S_0$-$3^3P_1$ | 1.10(0) | 1.77(0) | 2.27(0) | 5.53(0) | 1.07(1) |
| $2^1S_0$-$3^3P_2$ | 4.23(−1) | 1.80(−1) | 1.08(−1) | 5.29(−3) | |
| $2^1S_0$-$3^1S_0$ | 4.26(0) | 4.94(0) | 5.17(0) | 5.59(0) | 4.59(0) |
| $2^1S_0$-$3^1P_1$ | 2.82(0) | 5.03(0) | 6.60(0) | 1.64(1) | 3.19(1) |
| $2^1P_1$-$3^3S_1$ | 5.73(−1) | 4.01(−1) | 3.74(−1) | 7.36(−1) | 1.59(0) |
| $2^1P_1$-$3^3P_0$ | 4.29(−1) | 1.89(−1) | 1.16(−1) | 7.06(−3) | |
| $2^1P_1$-$3^3P_1$ | 1.41(0) | 1.09(0) | 1.03(0) | 4.66(−1) | 1.98(−1) |
| $2^1P_1$-$3^3P_2$ | 2.03(0) | 1.06(0) | 7.87(−1) | 2.03(−1) | 8.11(−2) |
| $2^1P_1$-$3^1S_0$ | 2.92(−1) | 5.51(−1) | 7.51(−1) | 2.28(0) | 4.79(0) |
| $2^1P_1$-$3^1P_1$ | 1.26(1) | 1.39(1) | 1.44(1) | 1.47(1) | 1.29(1) |
| $3^3S_1$-$3^3P_0$ | 3.48(2) | 6.51(2) | 7.19(2) | 9.45(2) | 1.14(3) |
| $3^3S_1$-$3^3P_1$ | 4.01(2) | 4.73(2) | 4.76(2) | 4.52(2) | 5.34(2) |
| $3^3S_1$-$3^3P_2$ | 1.06(3) | 2.35(3) | 2.69(3) | 3.79(3) | 4.74(3) |
| $3^3S_1$-$3^1S_0$ | 2.10(0) | 1.22(0) | 1.07(0) | 2.93(−1) | 4.23(−2) |
| $3^3S_1$-$3^1P_1$ | 1.44(2) | 3.20(2) | 3.67(2) | 5.23(2) | 6.59(2) |
| $3^3P_0$-$3^3P_1$ | 3.97(0) | 2.08(0) | 1.63(0) | 3.42(−1) | 4.76(−2) |
| $3^3P_0$-$3^3P_2$ | 3.58(1) | 3.10(1) | 2.88(1) | 1.22(1) | 4.67(0) |
| $3^3P_0$-$3^1S_0$ | 3.28(−1) | 7.76(−2) | 4.06(−2) | 1.76(−3) | |
| $3^3P_0$-$3^1P_1$ | 2.24(0) | 5.05(−1) | 2.49(−1) | 7.06(−3) | |
| $3^3P_1$-$3^3P_2$ | 6.76(1) | 5.47(1) | 5.03(1) | 2.10(0) | 8.04(0) |
| $3^3P_1$-$3^1S_0$ | 1.15(2) | 9.26(1) | 7.95(1) | 1.98(1) | 9.67(0) |
| $3^3P_1$-$3^1P_1$ | 4.57(1) | 3.81(1) | 3.53(1) | 1.49(1) | 5.70(0) |
| $3^3P_2$-$3^1S_0$ | 1.64(0) | 3.88(−1) | 2.01(−1) | 3.53(−3) | |
| $3^3P_2$-$3^1P_1$ | 2.77(1) | 2.06(1) | 1.87(1) | 7.25(0) | 2.59(0) |
| $3^1S_0$-$3^1P_1$ | 4.90(2) | 1.12(3) | 1.28(3) | 1.78(3) | 2.23(3) |

times threshold, these values yield $l_{\max} < 15$ for all ions. $l_{\max}$ is therefore set equal to 15 and the CB approximation is employed to obtain the contribution to collision strengths from the sum $\sum_{l=16}^{\infty} \Omega^l$. Atomic structure data given in Tables I and II is used for the calculations (as mentioned earlier, the NBS values are used for the oscillator strengths of iron). DW partial collision strengths were found to converge to the CB values at some $l' < l_{\max}$ for all cases where checks were made. It is also seen that the transitions from the ground state do not contain contributions from $l > l_{\max}$ until very high incident energies, where any error in $\Omega^l_{\mathrm{CB}}$, if present, would be small.

#### 4. *Transformation to intermediate coupling*

The *LS* reactance matrices computed in the DW or the CC approximations are transformed to IC (in a pair-coupling formulation) employing term-coupling coefficients obtained by diagonalizing the nonrelativistic and the Breit-Pauli parts of the total Hamiltonian. Partial IC collision strengths $\sum_{l=0}^{15} \Omega^l(\mathrm{IC})$ are computed by the method used by Saraph on summing over all contributing $LS\pi$ states in Eq. (5). The resulting total $J\pi$ states range from 0.5 to 16.5 for both parities. The majority of $J\pi$ states, from $J=2.5$ to 12.5, contain 33 channels in the pair-coupling scheme. As an example, in Table III we list these channels for one case, $J=2.5$ (odd parity), for scattering with $Mo^{40+}$. The ion energies listed are target term energies in *LS* coupling. Comparison with Table I shows that for an ion as highly charged as $Mo^{40+}$, these differ from the relativistic energies by a significant amount. In the present approach, the fine-structure level separations are considered to be small relative to the *LS* terms and all fine-structure states are taken to be of the same energy as the nonrelativistic term. For permitted transitions this approximation does not result in a large error so long as condition (12) is fulfilled (see Jones[12]). In the present calculations, there may therefore be some error in the collision strength at energies close to the excitation threshold although a specific determination of its magnitude was not made.

## IV. RESULTS AND DISCUSSION

The total nonresonant IC collision strengths for $Fe^{24+}$, $Se^{32+}$, and $Mo^{40+}$ are given in Tables IV, V, and VI,

respectively, for all transitions involving all states up to the $n=3$ levels including the fine structure. The collision strengths are multiplied by $Z^2$ and the incident electron energies $k_1^2$ (in Rydbergs, relative to the ground state) have been divided by $Z^2$ in order to emphasize the obvious scaling of these two quantities with $Z$. The incident energies were chosen so as to bring out some structure in a few transitions such as $1^1S_0$-$2^3P_1$ (see below). In principle, all transitions *not* affected by IC, i.e., those involving the levels $n^{3,1}P_1$, should correspond to the same scaled collision strength. Thus the spread in $Z^2\Omega$ for such transitions (e.g., $1^1S_0$-$2^3S_1$) is an indication of the error in the present calculations. Comparing the values for all transitions at the first scaled energy (approximately the same for the three ions), we find that the maximum spread is about 18% for the transition $2^3P_0$-$3^3P_0$. We expect that, in general, the error should be about 5—10% which is the spread found for most of the non-IC transitions. In fact, it is somewhat remarkable that the differences in $Z^2\Omega$ are not larger than we find, since the calculations are independently carried out for each ion and involve a number of steps with potential numerical errors (in particular, the summation for about 80 total $SL\pi$ states). Although it is not possible to go into the details of the computational techniques, the size and scope of the present calculations provides a useful check on the methods employed in a number of different ways; for example, the choice of internal integration mesh, the sensitivity to variational parameters in the TFD potential, the precision at very high scattering energies (where the relevant matrix elements are small), etc.

In order to interpolate or extrapolate the collision strengths to other $Z$ values we recommend that the mean $Z^2\Omega$ of the three values, in Tables IV—VI, for each transition (non-IC type) and energy be used. Some of the transitions are of special interest for a variety of reasons. These are discussed in Sec. IV A.

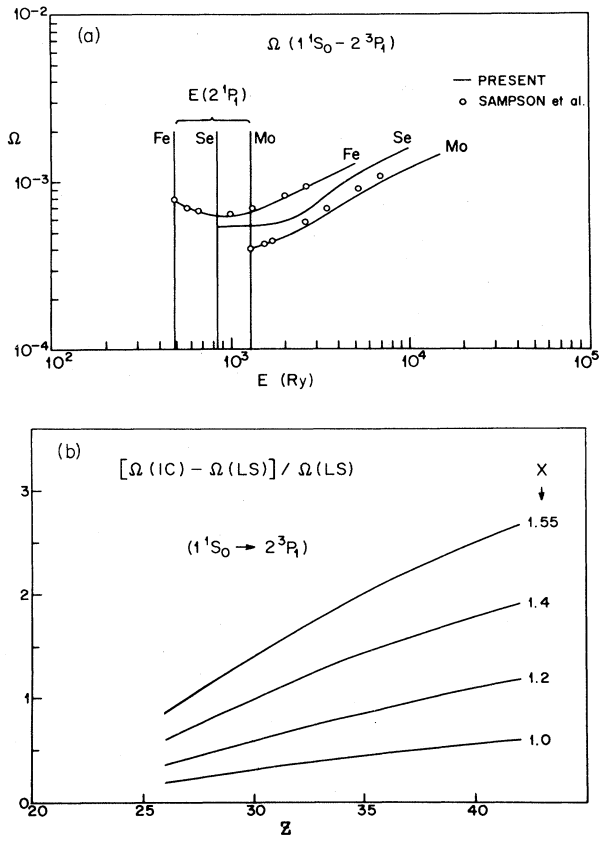


FIG 2. (a) Collision strengths for the transitions $1^1S_0$-$2^3P_1$ in $Fe^{24+}$, $Se^{32+}$, and $Mo^{40+}$. (b) Departure from $LS$ coupling with ion charge and incident electron energy (in threshold units).

### A. Particular features of some transitions

We now have the following:

$1^1S_0$-$2^3P_1$. This is an intercombination-type transition of considerable importance in the observed spectra of He-like ions (where it is commonly designated by the letter $y$). For ions with lower $Z$ ($Z<20$), the collision strength may be calculated in $LS$ coupling. However, as the spin-orbit coupling becomes stronger with $Z$ there is increasing deviation from the $LS$ scheme and the transition becomes more and more like an optically allowed one in the IC scheme. In Fig. 2(a) we plot $\Omega(1^1S_0$-$2^3P_1)$ for $Fe^{24+}$, $Se^{32+}$, and $Mo^{40+}$ at energies from threshold up to values where the Bethe form for allowed transitions becomes evident, i.e., $\Omega \sim \ln\epsilon$. The log-log plot shows a straight line behavior at high energies (circles are the calculations by Sampson, Parks, and Clark[22]). At lower energies we find different structure in the collision strengths for the three ions. In $Fe^{24+}$ it is clear that the contribution from high partial waves manifests itself only at energies about two times above threshold and until then the collision strength behaves in a monotonically decreasing manner like a semiforbidden transition. As the ion charge increases the relativistic effects get stronger and, for $Mo^{40+}$, $\Omega(1^1S_0$-$2^3P_1)$ is nearly a completely optically allowed transition with only a slight inflection at energies close to threshold. We further study the departure from $LS$ coupling in $\Omega(1^1S_0-2^3P_1)$, with $Z$, by plotting Fig. 2(b) where the ratio $[\Omega(\mathrm{IC})$-$\Omega(LS)]/\Omega(LS)$ is given at various energies $X$, in threshold units. As we know, $Z^2\Omega(LS)$ is constant with $Z$ and therefore, knowing the $LS$ collision strength and the ratio from Fig. 2(b), one may obtain $\Omega$(IC) for any ion up to about $Z=45$ to energies corresponding to $X \simeq 1.6$. It is seen that for $Fe^{24+}$, at threshold, $\Omega$(IC) is about 18% larger than $\Omega(LS)$. For $Ca^{18+}$ the corresponding increase is negligible, although at higher energies the collision strength is affected. $Z^2\Omega(LS)$ at energies $X=1.0$, 1.6, and 2.2 is approximately 1.30, 0.65, and 0.20, respectively.

$2^3S_1$-$2^1P_1$. This transition exhibits a very large IC effect. In Fig. 3 we have plotted the contribution to the collision strength from $l,l' \leq 15$ for $Fe^{24+}$ and $Mo^{40+}$ in $LS$ and IC coupling. The difference between the $LS$ and the IC is up to a few orders of magnitude at higher energies. In fact, the IC collision strength would be enhanced further if we were to include the CB contribution from $l>15$ as well [the total $\Omega$(IC) is given in Tables IV—VI]. The change in the transition from an $LS$ forbidden to IC al-

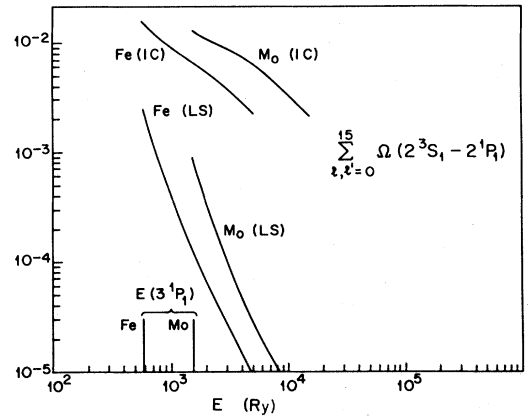


FIG. 3. *LS* and *IC* collision strengths for the transition $2^3S_1$-$2^1P_1$, summed over the first 15 partial waves, for $Fe^{24+}$ and $Mo^{40+}$.

lowed has interesting implications in the resonance enhancement in the collision strength for this transition found by PNH. We had calculated earlier that in *LS* coupling the rate parameter $\gamma(2^1P \rightarrow 2^3S)$ would be enhanced by up to about a factor of 5 due to resonances at $10^7$ K in $Fe^{24+}$. However, in IC the transition is found to be a strong optically allowed one and the background scattering cross section is much larger than before. Therefore the *relative* enhancement due to resonances is expected to be much smaller. In paper II we give the IC and the resonance contributions.

$n\,^1S_0 - n'\,^1S_0$. The term-coupling coefficients, as defined in Eq. (7), depend on the coefficients of diagonalization of the nonrelativistic Hamiltonian as well as the Breit-Pauli Hamiltonian, which includes one-body operators (mass-variation and the Darwin terms). Thus, configuration interaction between different complexes affects the total eigenfunction representation of states $n\,^1S_0$ through mixing between the three configurations $1s^2$, $1s\,2s$, and $1s\,3s$. Differences are therefore found between the *LS* and the IC values for transitions $1^1S_0$-$2^1S_0$, $1^1S_0$-$3^1S_0$, and $2^1S_0$-$3^1S_0$. This problem has been commented upon by Jones[12] and by Sampson *et al.*[22] Since there are no fine-structure type interactions that would cause the differences, we think it is more accurate to substitute the *LS* values for these three transitions in Tables IV—VI (as has been done). Sampson *et al.* do not allow for configuration mixing between the states involved and therefore their *LS* and IC values are identical and are found to be in reasonable agreement with the present *LS* values (see Table VII).

$2^3P_1$-$2^1S_0$. Sampson and Clark[14] found a large discrepancy for this transition between their calculations and those of Jones[12] for $Fe^{24+}$. The present value (Table VII) is fairly close to the former, confirming that Jones's value [9.83(−3) at 676 rydbergs] is in error. Jones's calculations for the lower partial waves extended up to $l=9$ whereas the present ones go up to $l=15$. We are not therefore able to isolate precisely the cause of the error, but it appears that it lies mainly in the CB summation where Jones's line strength is approximately a factor of 2 lower compared with the present one (see Table II), which is in agreement with that of Sampson and Clark. Our

TABLE VII. Comparison of nonresonant collision strengths with earlier calculations.

| | | $Z=26$ | | | | $Z=42$ | |
|---|---|---|---|---|---|---|---|
| Transition | $X$[a] | $\Omega^P$[b] | $\Omega^J$[c] | $\Omega^{SPC,SC}$[d] | | $\Omega^P$ | $\Omega^{SPC}$ |
| $1^1S_0$-$2^3S_1$ | 1.4 | 2.42(−4) | 2.37(−4) | 2.48(−4) | 1.2 | 1.06(−4) | 1.11(−4) |
| $1^1S_0$-$2^1S_0$ | 1.4 | 7.45(−4) | 7.34(−4) | 8.94(−4) | 1.2 | 2.05(−4) | 2.84(−4) |
| $1^1S_0$-$2^1S_0(LS)$ | 1.4 | 8.42(−4) | | 8.94(−4) | 1.2 | 2.62(−4) | 2.84(−4) |
| $1^1S_0$-$2^1P_1$ | 1.4 | 3.45(−3) | 3.44(−3) | 3.77(−3) | 1.33 | 1.04(−3) | 1.18(−3) |
| $1^1S_0$-$2^1P_1(LS)$ | 1.4 | 3.81(−3) | 3.78(−3) | 4.05(−3) | 1.33 | 1.48(−3) | 1.45(−3) |
| $1^1S_0$-$3^3P_1$ | 1.0 | 2.78(−1) | | 2.65(−1) | 1.0 | 1.81(−5) | 8.84(−5) |
| $1^1S_0$-$3^3P_1$ | 4.0 | 1.11(0) | | 1.17(0) | 4.0 | 1.47(−4) | 1.76(−4) |
| $2^3P_1$-$2^1P_1$ | 1.4 | 1.55(−2) | 1.36(−2) | 1.52(−2) | | | |
| $2^3P_1$-$2^3P_1$ | 1.4 | 3.87(−3) | 3.77(−3) | 4.15(−3) | | | |
| $2^3P_0$-$2^3P_2$ | 1.4 | 6.94(−3) | 6.45(−3) | 6.66(−3) | | | |
| $2^3P_1$-$2^3P_2$ | 1.4 | 1.86(−2) | 1.74(−2) | 1.82(−2) | | | |
| $2^3P_1$-$2^1S_0$ | 1.4 | 7.00(−2) | 9.83(−3) | 7.45(−2) | | | |
| $2^3P_2$-$2^1S_0$ | 1.4 | 1.04(−3) | 7.71(−4) | 8.51(−4) | | | |
| $2^3S_1$-$2^3P_1$ | 1.4 | 3.78(−1) | 3.93(−1) | 3.89(−1) | | | |
| $2^3S_1$-$2^1S_0$ | 1.4 | 1.36(−3) | 1.33(−3) | 1.41(−3) | | | |
| $2^3S_1$-$3^3P_1$ | 1.0 | 5.18(−3) | | 5.53(−3) | 1.0 | 1.90(−3) | 1.84(−3) |
| $2^1S_0$-$3^1P_1$ | 1.0 | 4.58(−3) | | 4.73(−3) | 1.0 | 1.60(−3) | 1.54(−3) |
| $2^3S_1$-$3^1P_1$ | 1.0 | 1.54(−3) | | 1.61(−3) | 1.0 | 8.62(−4) | 8.90(−4) |
| $2^3P_1$-$3^3S_1$ | 1.0 | 1.02(−3) | | 1.06(−3) | 1.0 | 3.74(−4) | 3.93(−4) |

[a] $X$ is in threshold units.
[b] $P$, present work.
[c] J, Jones (Ref. 12).
[d] SPC, Sampson, Parks, and Clark (Ref. 21); SC, Sampson and Clark [Ref. 14, approximation $p\,2$, Eq. (66)].

partial collision strengths, at 676 rydbergs above the ground state, are 1.10(−2) and 5.79 for $\sum_{l=0}^{15}$ and $\sum_{l=15}^{30}\infty$, respectively, compared with 6.44(−3) and 3.39(−3) for $\sum_{l=0}^{9}$ and $\sum_{l=9}^{\infty}$ obtained by Jones.

$2^3S_1-2^3P_J$. We expect some significant differences between the present IC calculations and our previous $LS$ calculations (PNH). In the $LS$ scheme we obtained the $f$ values for $2^2S$-$2^3P$, upon $Z$ extrapolation from $Z<10$, to be 2.73(−2), 2.06(−2), and 1.66(−2) for $Fe^{24+}$, $Se^{32+}$, and $Mo^{40+}$, respectively. These values (quite different from the ones in Table II) were used by PNH to sum over the large contribution from $l>15$. The present results, summed over the fine structure, i.e., $\sum_{J=0}^{2}\Omega(2^3S_1$-$2^3P_J)$, are 1.02(0), 5.50(−1), and 3.37(−1), respectively, for the three ions at $X\simeq 1.2$ in threshold units. The PNH values at the same energy for $\Omega(2^3S-2^3P)$ are 1.18(0), 7.20(−1), and 4.90(−1), respectively. Of course, the differences between the two calculations are larger, in percentage terms, if the fine-structure collision strengths are compared with the ones obtained from the $LS$ collision strengths with simple statistical weight assignments.

$1^1S_0$-$3^3P_1$. In Fig. 4 we plot the collision strengths for this transition for all three ions and compare with the calculations for $Fe^{24+}$ and $Mo^{40+}$ by Sampson *et al.*[22] The difference between the two sets of results is larger than for $1^1S_0$-$2^3P_1$, particularly in the high-energy region for $Mo^{40+}$. The discrepancies are probably due to different oscillator strengths used for the contribution from the high partial waves. In the case of $Mo^{40+}$ some difference is also found in the region just above threshold, arising from the contribution from low partial waves. The maximum discrepancy is about 12% at the last point of comparison in $Mo^{40+}$.

### B. Previous calculations

The two sets of calculations[12,14,22] already mentioned are available for detailed comparison for a number of transitions considered here. In Table VII we select and present a few of these according to the different types of transitions, i.e., from the ground state, $\Delta n=0$, $\Delta n\neq 0$, etc. Also, the comparison is made at different energies (in threshold units) for $Fe^{24+}$ and $Mo^{40+}$. The overall agreement is fairly close, confirming the expectation that for ions as highly charged as these, the Coulomb-Born approximation (used in Refs. 14 and 22) and the DW (used in Ref. 12 and the present work), yield similar results. The high partial waves for optically allowed transitions are treated in the CB approximation in all calculations. The one difference that exists between the different sets of calculations is due to different eigenfunction representations. Here again, the final effect on the collision strengths is slight, since configuration interaction diminishes as the ion charge increases.

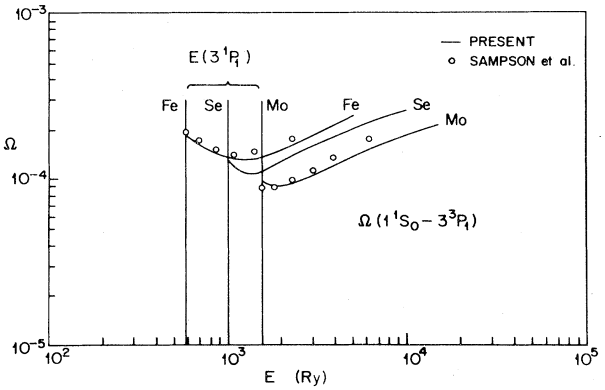


FIG. 4. Collision strengths for the transition $1^1S_0$-$3^3P_1$ in $Fe^{24+}$, $Se^{32+}$, and $Mo^{40+}$.

## V. CONCLUSION

Nonresonant IC collision strengths are computed for $Fe^{24+}$, $Se^{32+}$, and $Mo^{40+}$ in a 9 DW approximation. Close-coupling calculations were also found to agree with the DW ones for $l\leq 4$ showing that, even for low partial waves and near threshold energies, the coupling effects on the background excitation cross sections are negligible (the CC and the DW results are too close to be given for detailed comparison). There is good agreement between the results presented here and available earlier calculations. However, the aim of the calculations reported here in paper I is not merely to compute IC collision strengths (although these in themselves should be useful for practical applications for a number of transitions), or to provide a check on previous such work, but also to obtain scattering matrices in order to analyze detailed resonance effects in highly charged ions that are now known to be important, and to incorporate these in the total scattering calculations. That is the subject of paper II.

## ACKNOWLEDGMENTS

The present work (papers I and II) is based on theoretical and computational techniques developed by, or under the guidance of Professor M. J. Seaton. The author is privileged to have spent a few years working with Professor Seaton at University College London, and it is a great pleasure to acknowledge his many valuable contributions to this work. $LS$ coupling calculations (unpublished) in a five-state DW approximation were earlier carried out by Dr. David Norcross and Dr. David Hummer at the Joint Institute for Laboratory Astrophysics, Boulder, Colorado. This work was carried out under the auspices of the Natural Sciences and Engineering Research Council (NSERC) of Canada and the author is a recipient of the NSERC University Research Fellowhip award.

*Present address: Joint Institute for Laboratory Astrophysics, University of Colorado and National Bureau of Standards, Boulder, Colorado 80309.

[1]D. L. McKenzie and P. B. Landecker, Astrophys. J. 259, 372 (1982).
[2]E. Källne, J. Källne, and A. K. Pradhan, Phys. Rev. A 27, 1476 (1983).
[3]M. Bitter, S. Von Goeler, K. W. Hill, R. Horton, D. Johnson, W. Roney, N. Santhoff, E. Silver, and W. Stodiek, Phys. Rev. Lett. 47, 921 (1981).
[4]A. K. Pradhan, D. W. Norcross, and D. G. Hummer, Phys. Rev. A 23, 619 (1981).
[5]A. K. Pradhan, Phys. Rev. Lett. 47, 79 (1981).
[6]W. Eissner and M. J. Seaton, J. Phys. B 5, 2187 (1972).
[7]M. J. Seaton, J. Phys. B 7, 1817 (1974).
[8]P. G. Burke and M. J. Seaton, Methods Comput. Phys. 10, 1 (1971).
[9]W. Eissner, M. Jones, and H. Nussbaumer, Comput. Phys. Commun. 8, 270 (1974).
[10]H. E. Saraph, Comput. Phys. Commun. 15, 247 (1978); 3, 256 (1972).
[11]M. A. Hayes and M. J. Seaton, J. Phys. B 11, L79 (1978).
[12]M. Jones, Mon. Not. R. Astron. Soc. 169, 211 (1974).
[13]A. M. Ermolaev and M. Jones, J. Phys. B 7, 199 (1974).
[14]Douglas H. Sampson and Robert E. H. Clark, Astrophys. J. 44, 169 (1980).
[15]G. W. F. Drake, Phys. Rev. A 19, 1387 (1979).
[16]C. D. Lin, W. R. Johnson, and A. Dalgarno, Phys. Rev. A 15, 154 (1977).
[17]M. A. Crees, M. J. Seaton, and P. M. H. Wilson, Comput. Phys. Commun. 15, 23 (1978).
[18]A. Burgess and V. B. Sheorey, J. Phys. B 7, 2403 (1974).
[19]A. Burgess, J. Phys. B 7, L364 (1974).
[20]A. Burgess and J. A. Tully, J. Phys. B 11, 4271 (1978).
[21]M. J. Seaton, Adv. Atom. Mol. Phys. 11, 83 (1975).
[22]Douglas H. Sampson, Allen D. Parks, and Robert E. H. Clark, Phys. Rev. A 17, 1619 (1978).